SUPPLEMENTARY MATERIAL

Jin et al.

5-hydroxymethylcytosine is strongly depleted in human cancers but its levels do not correlate with IDH1 mutations

SUPPLEMENTARY FIGURES

Supplementary Fig. 1:

Analysis of 5hmdC by LC-MS/MS. A. The reaction pathway from cytosine (C) to 5-methylcytosine (5mC) and 5-hydroxymethylcytosine (5hmC) is shown. **B.** Typical selected-ion chromatograms (SICs) for monitoring 5hmdC (a), 5mdC (c) and dG (d) derived from a digested DNA sample of normal human brain DNA mixed with the two stable isotope labeled standards of 5hmdC (b) and dG (e). Shown in the inserts are chemical structures for each nucleoside and corresponding SRM transition in the TSQ mass spectrometer; the stable isotope labels are indicated in red atom characters.

Supplementary Fig. 2:

Mass calibration curves. An 897-bp DNA standard containing 100% 5hmdC (Zymo Research; Irvine, CA) was used to generate the mass calibration curves for labeled and corresponding unlabeled nucleosides of 5hmdC and dG. The same amount of labeled 5hmdC and dG standards as used in sample analysis were mixed with different concentrations of digested DNA standard. The peak area ratios of labeled and unlabeled deoxynucleosides of the LC-MS/MS measurements were calibrated to the actual quantity ratios of deoxynucleosides in the standard mixture. In addition, we used an 897-bp DNA standard containing 100% 5-mdC (Zymo Research) to construct the calibration curve of 5mdC using labeled dG as the standard. The peak area ratios of 5mdC to labeled dG were calibrated to the actual ratios of deoxynucleosides in the standards mixture. The ratios of unlabeled versus labeled

standards were chosen to be in the expected range of the sample deoxynucleoside. Linear equations were used for calculation of the precise 5hmdC, 5mdC and dG quantities in the samples; 5hmdC vs dG and 5mdC vs dG were used to present 5hmdC and 5mdC levels of the samples. We have chosen dG as a baseline standard, because it pairs with all three 2'-deoxycytidine derivatives: dC, 5mdC and 5hmdC. All calibration curves were constructed with three independent measurements. Calibration curves for normal 5hmdC vs labeled 5hmdC (a), normal dG vs labeled dG (b) and normal 5mdC vs labeled dG (c) measured by the TSQ mass spectrometer are shown.

Supplementary Fig. 3:

Quantitation of 5hmdC in various mouse and human tissues and cell types.

A. 5hmdC was measured in DNA from mouse sperm, mouse embryonic stem cells, mouse brain, human brain, the 293T cell line, a small cell lung cancer cell line, and in human fibroblasts. **B.** Measurement of 5mdC in the same samples. All assays were done in triplicate.

Supplementary Fig. 4:

Immuno dot blot analysis of 5hmC in normal brain and brain tumors. Normal brain DNA from prefrontal cortex and DNA from brain tumors (200 ng each) were spotted onto nylon membranes, which were probed with anti-5hmC or anti-5mC antibody as described in Jin et al. (2011) Nucleic Acids Res 39: 5015-5024. The samples were analyzed by LC-MS/MS (Fig. 2).

Supplementary Fig. 5:

Quantitation of 5hmdC and 5mdC in lung small cell carcinomas and adenocarcinomas. A. 5hmdC levels in primary small cell lung cancer. N, normal

lung; T, small cell lung cancer. **B.** 5mdC levels in primary small cell lung cancer. **C.** 5hmdC levels in lung adenocarcinomas. LN, normal lung; LT, lung tumor. **D.** 5mdC levels in lung adenocarcinomas. The analysis was performed by LC-MS/MS as described in Materials and Methods.

Supplementary Fig. 6:

Quantitation of 5hmdC and 5mdC in neurons and astrocytes of human fetal brain. A. 5hmdC**. B.** 5mdC**.** The analysis was performed by LC-MS/MS as described in Materials and Methods.

Supplementary Fig. 7:

IDH1 **and** ***IDH2*** **mutations in brain and lung tumor samples. A. Sequencing scans.** The sequences show a wildtype sequence, the common IDH1 R132H mutation, a minor allele fraction of R132H in tumor BT26 and a mutation IDH1 R132G in tumor BT25. **B.** Summary of the mutation status of IDH1/2 in lung and brain tumors. Mutations of IDH2 in brain tumors are extremely rare and were not determined (N.D.).

Supplementary Fig. 8:

Model for inhibition of TET oxidase activity and 5hmC production by the oncometabolite 2-hydroxyglutarate (2HG) produced by mutant IDH1.

Supplementary Fig. 9:

Immunohistochemical analysis of 5hmC on additional human tissue arrays. Human tissue arrays containing paired samples of malignant tumor and corresponding normal tissue (breast, colon, skeletal muscle, stomach, prostate, ovary) were stained with anti-5hmC antibody and detected with secondary antibody

conjugated to Rhod Red-X-AffiniPure. The magnification of all panels is 10-fold. Hoechst 33258 staining (blue) is shown as a control.

Supplementary Fig. 10:

Analysis of additional lung tumors. A. 5hmC staining of additional lung squamous cell (SCC) and adenocarcinomas. Results are shown for matched pairs of tumor-adjacent normal tissue and two squamous cell carcinomas (sample 509019, panels a and b; sample B509018, panels c, d, and e) and two adenocarcinomas (sample B509016, panels f and g; sample B509015; panels h, i, and j). Boundary sections between normal and tumor are also shown (panels d and i). **B.** Comparison of 5hmC and Ki67 staining in normal lung and in SCC lung tumors. The staining for 5hmC and Ki67 is mutually exclusive. Red, 5hmC; green, Ki67. All Ki67-positive cells lack 5hmC staining.

Supplementary Fig. 11:

Co-staining with anti-5hmC and anti-5mC antibodies. A. Normal brain section and brain tumor; **B.** Normal liver and liver tumor. **C.** Normal kidney and kidney tumor.

Supplementary Fig. 12:

5hmC and Ki67 antigen in brain and brain tumors. A. Ki67 staining of normal brain sections and brain tumors shows absence of Ki67 staining in normal brain**. B.** Mostly mutually exclusive staining for Ki67 and 5hmC in brain tumors. Data for two brain tumors are shown.

Supplementary Fig. 13:

Analysis of 5hmC and Ki67 in uterus, breast and pancreas tissue and tumors. Red, 5hmC; green, Ki67. Ki67-positive cells lack 5hmC staining. Note that not all cells that lack 5hmC staining in the tumors are Ki67-positive presumably due to past history of proliferation leading to persistent loss of 5hmC.

Supplementary Fig. 14:

Expression of the *TET1*, *TET2*, and *TET3* genes in normal brain and astrocytic gliomas and in normal lung and lung squamous cell carcinomas. A. Brain. BN, normal brain; BT, brain tumor. **B.** Lung. LN, normal lung; LT, lung tumor. Gene-specific RT-PCR data for all three *TET* genes were normalized to beta-actin levels. PCR was performed with the TaqMan MGB primer with 6FAM-based probes (Applied Biosystems) using the following assay ID numbers: TET1 (Hs00286756_m1), TET2 (Hs00325999_m1), TET3 (Hs00379125_m1). Although expression levels of certain *TET* genes were higher in some tumors than in corresponding normal tissue, no generalized trend was observed. Overall, *TET* expression levels were not reduced in tumors, and there was no correlation between *TET* expression and levels of 5hmdC (Figs. 1 and 2).

A

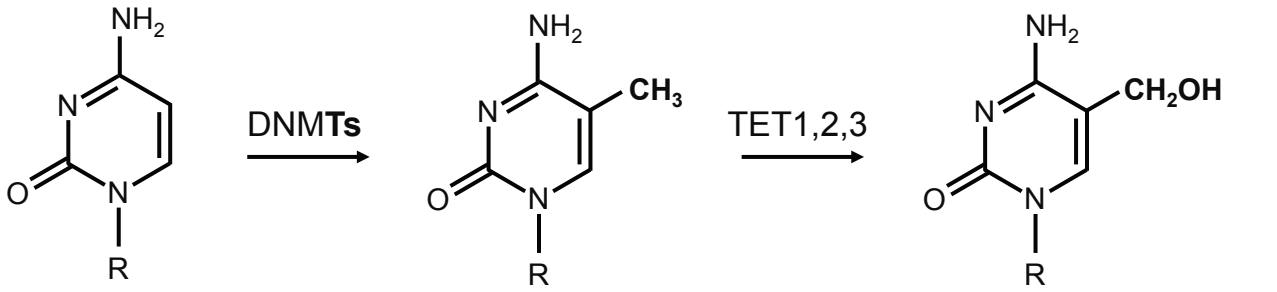

cytosine (C) 5-methylcytosine (5mC) 5-hydroxymethylcytosine (5hmC)

B

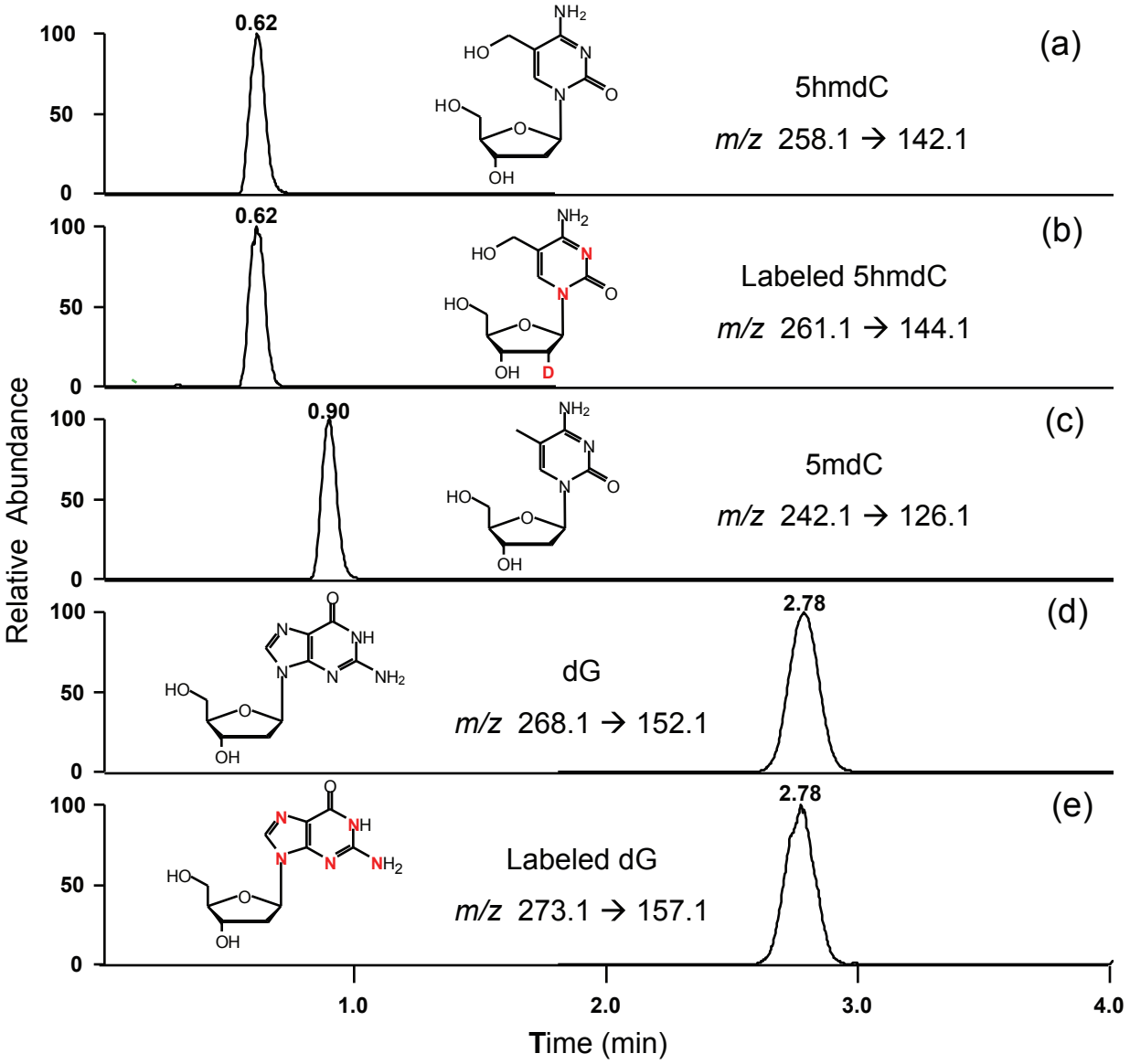

Suppl. Fig. 1

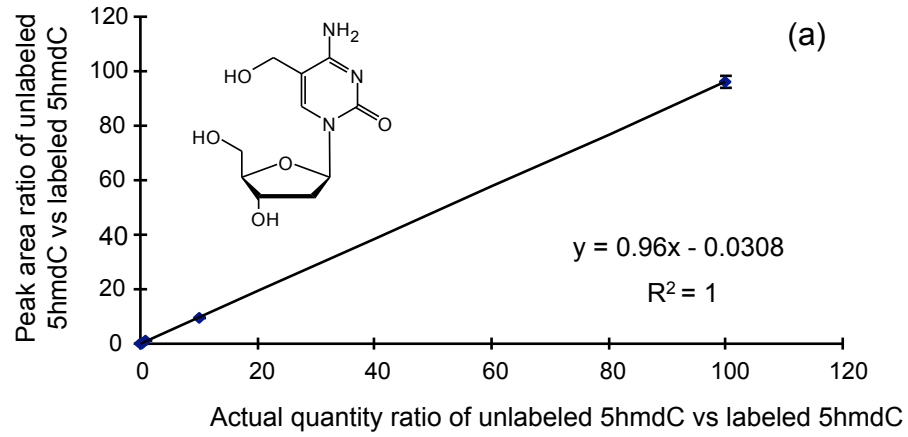

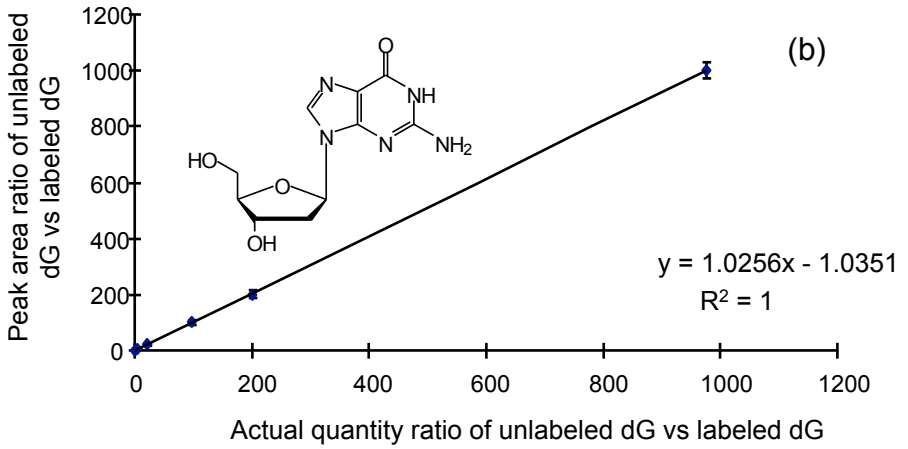

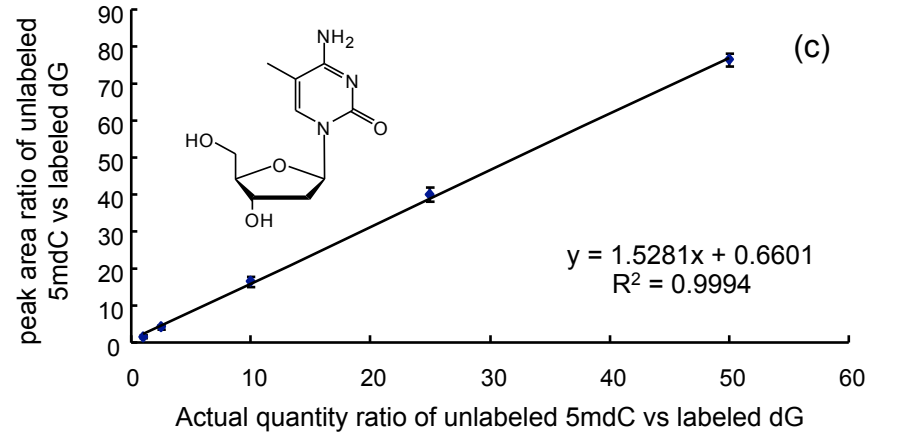

Supplementary Fig. S2

A

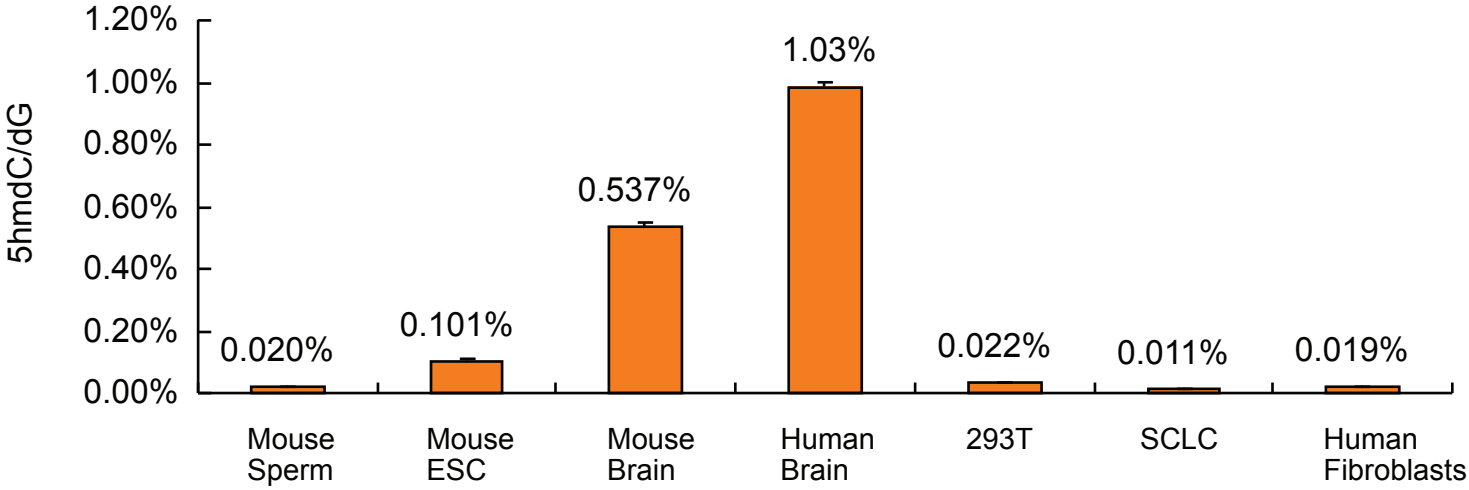

B

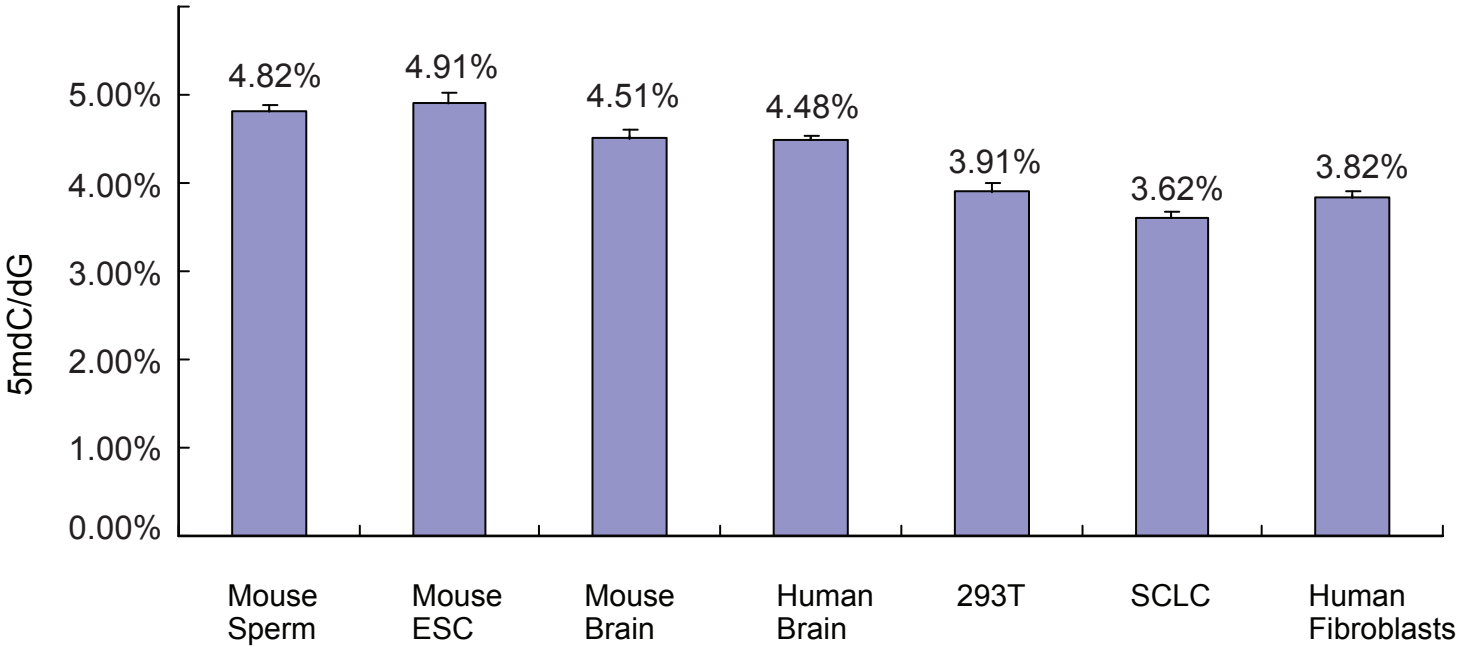

Supplementary Fig. S3

A

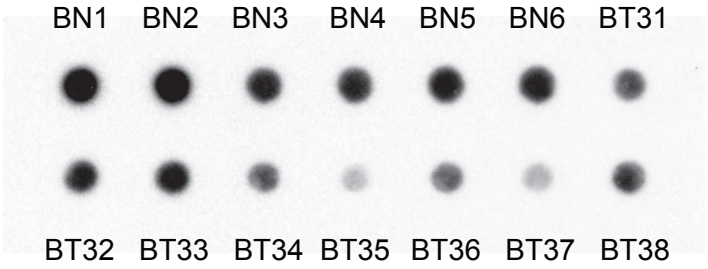

anti-5hmC antibody

B

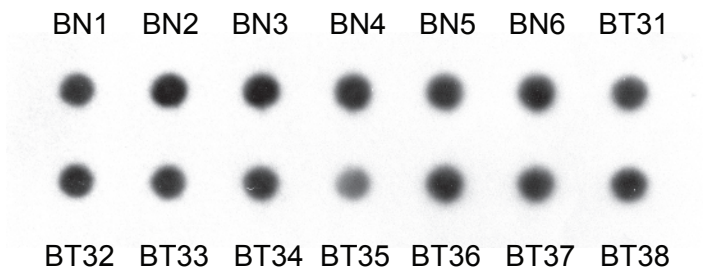

anti-5mC antibody

Supplementary Fig. S4

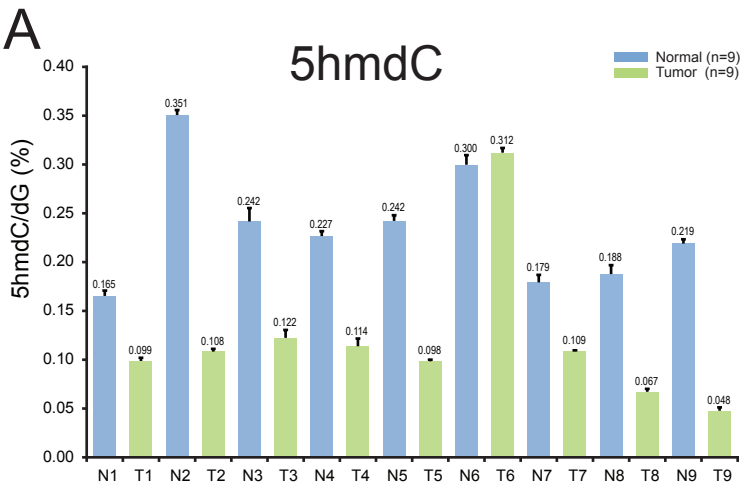

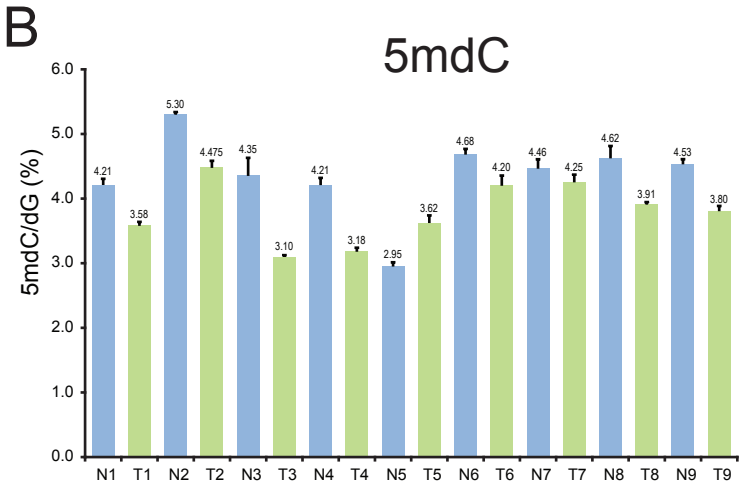

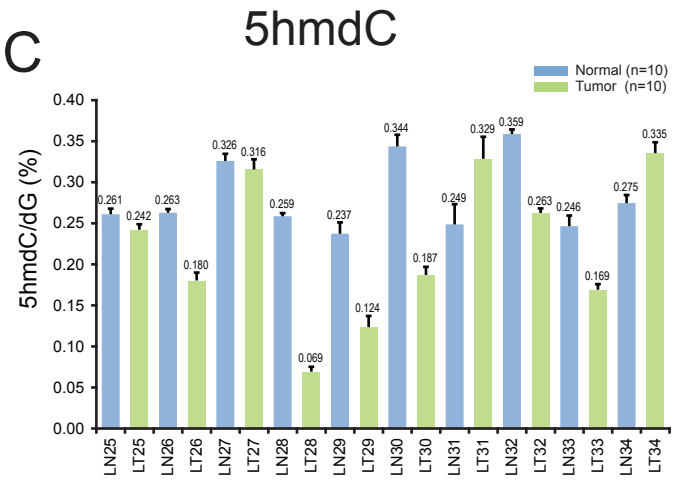

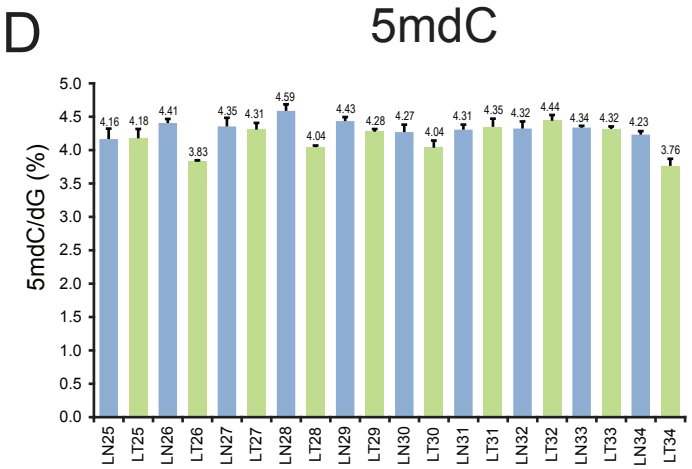

Supplementary Fig. S5

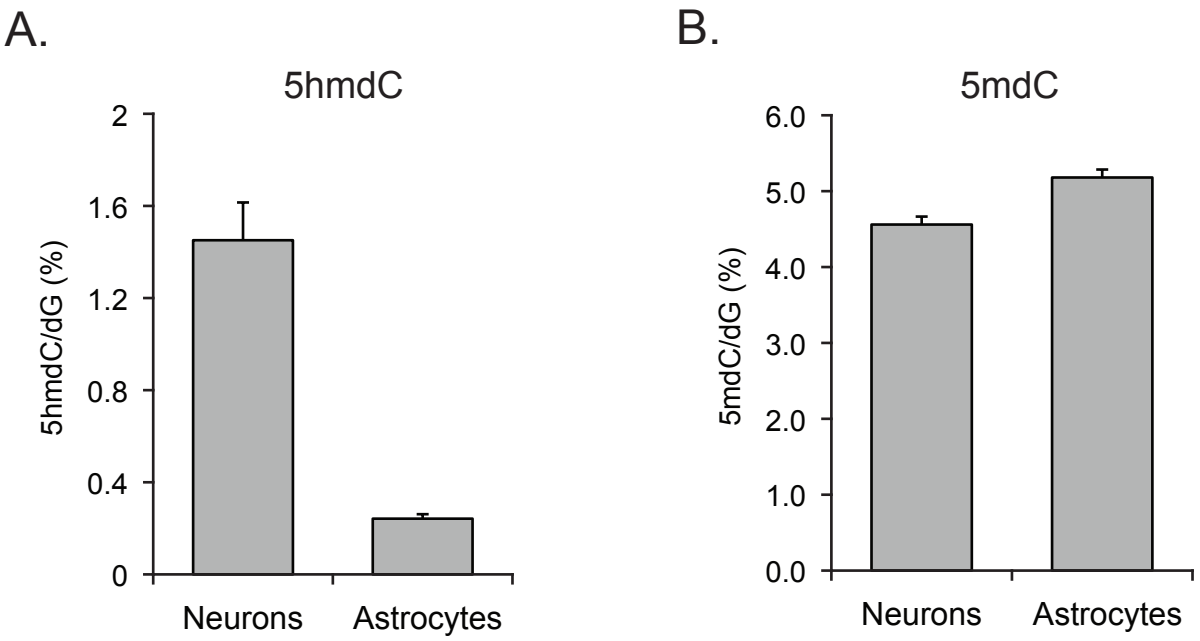

Supplementary Fig. S6

A

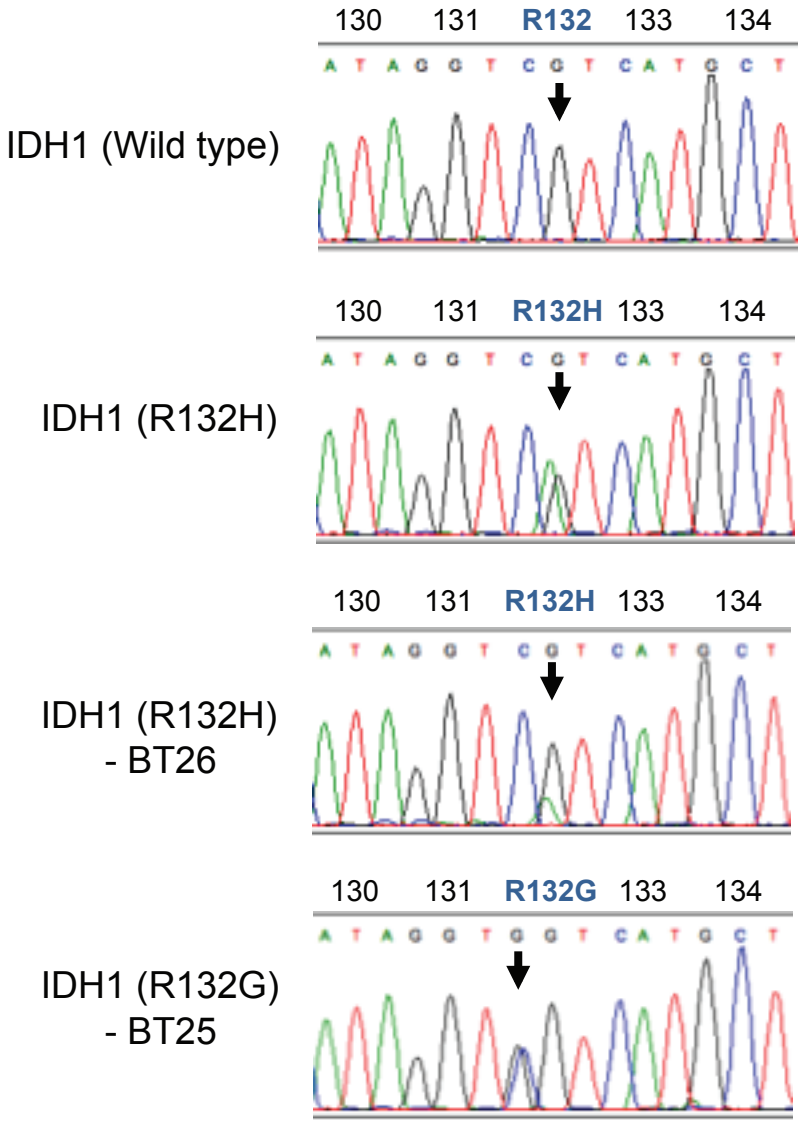

B

Tissue		Number of Samples	*IDH1* mutations		*IDH2* mutations	
			Number	%	Number	%
Brain	Normal	6	0	0	N.D.	N.D.
	Tumor	39	19	48.7	N.D.	N.D.
Lung (SCC)	Normal	18	0	0	0	0
	Tumor	24	0	0	0	0

Supplementary Fig. S7

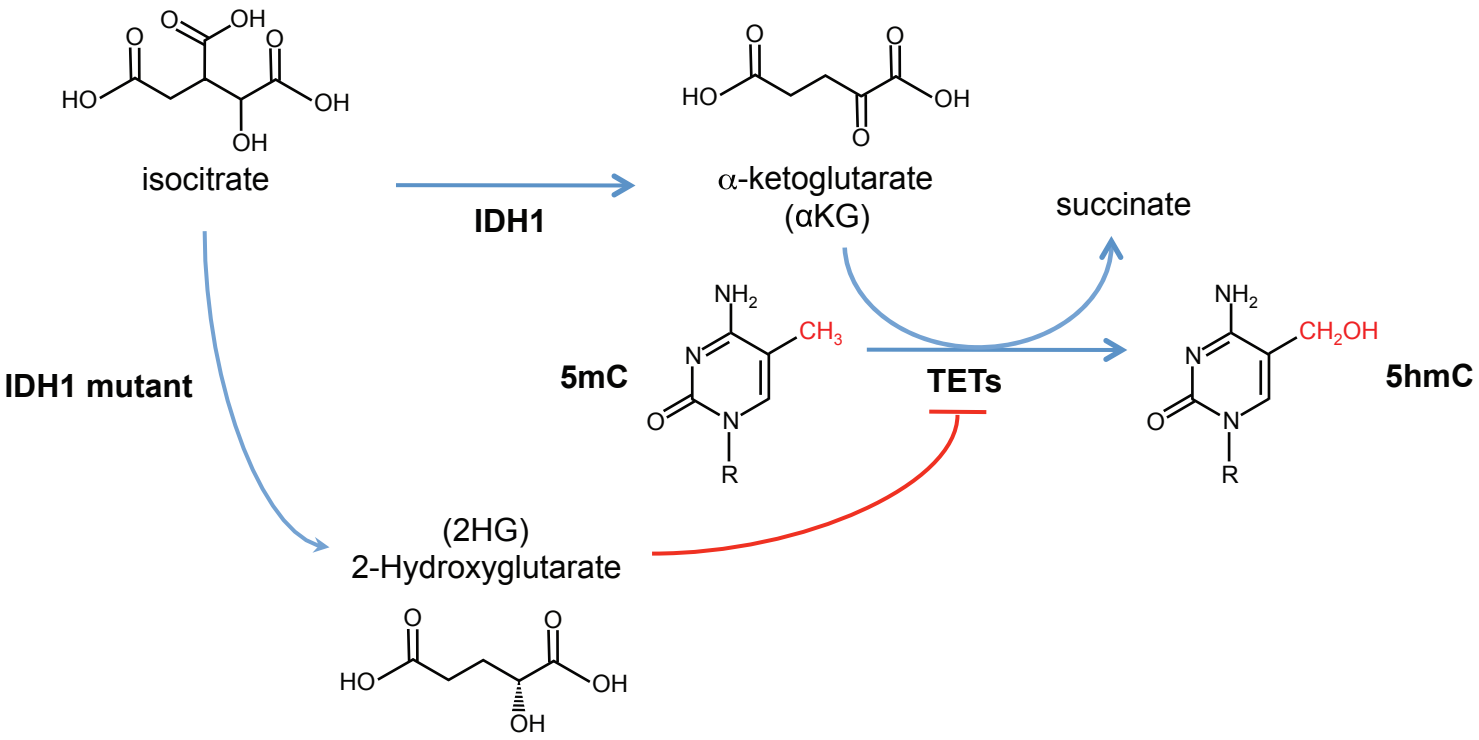

Supplementary Fig. S8

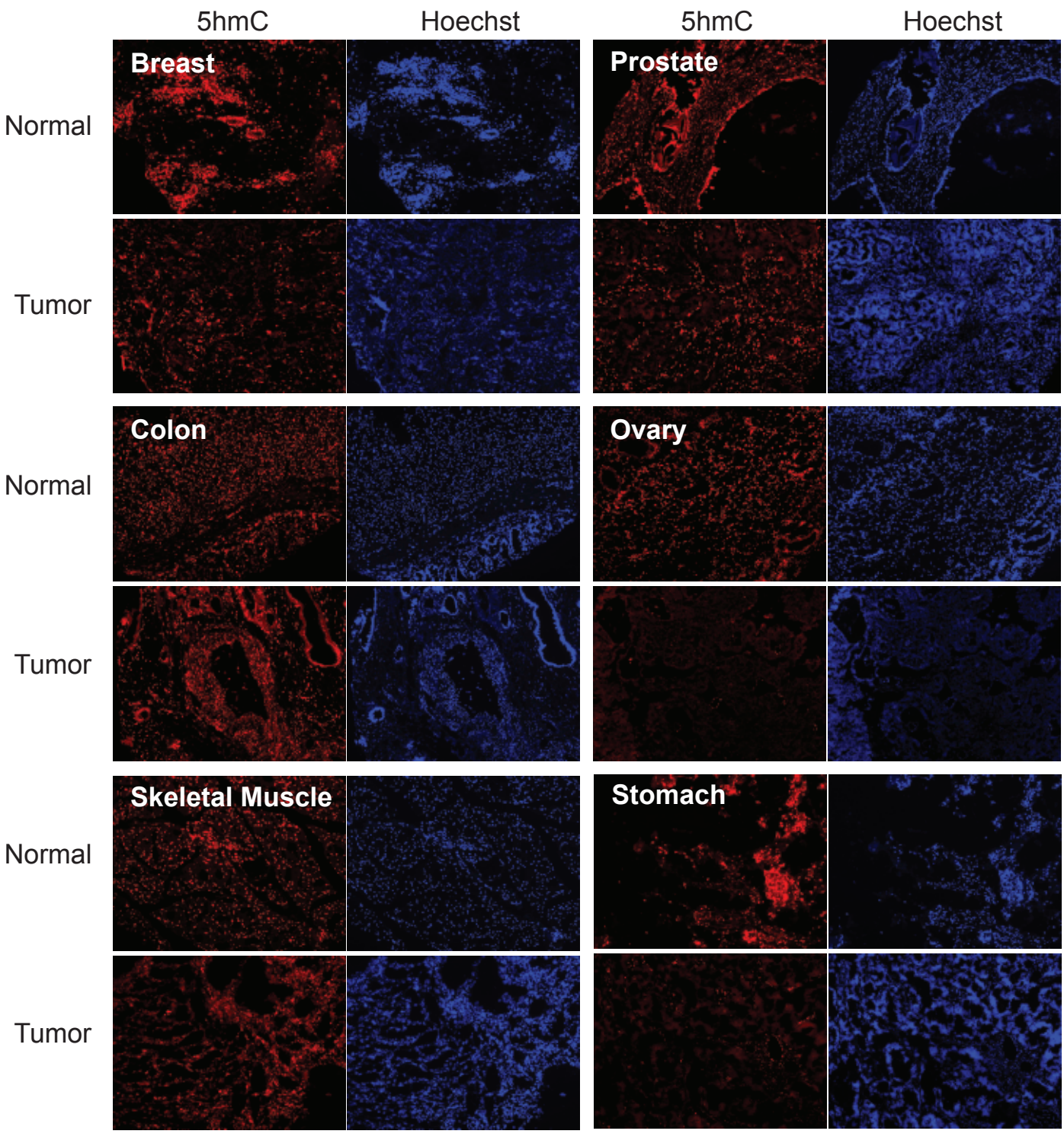

Supplememtary Fig. S9

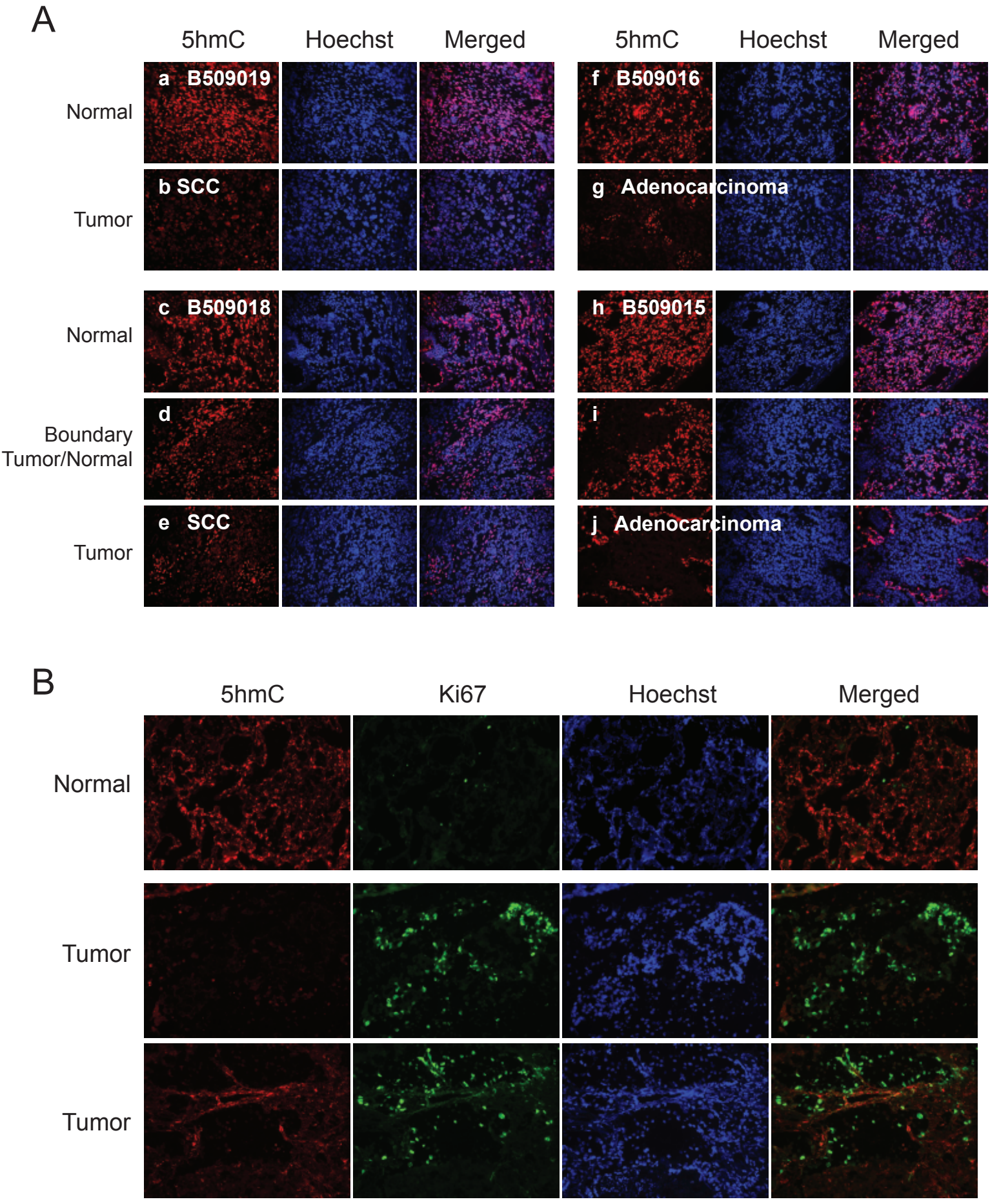

Supplememtary Fig. S10

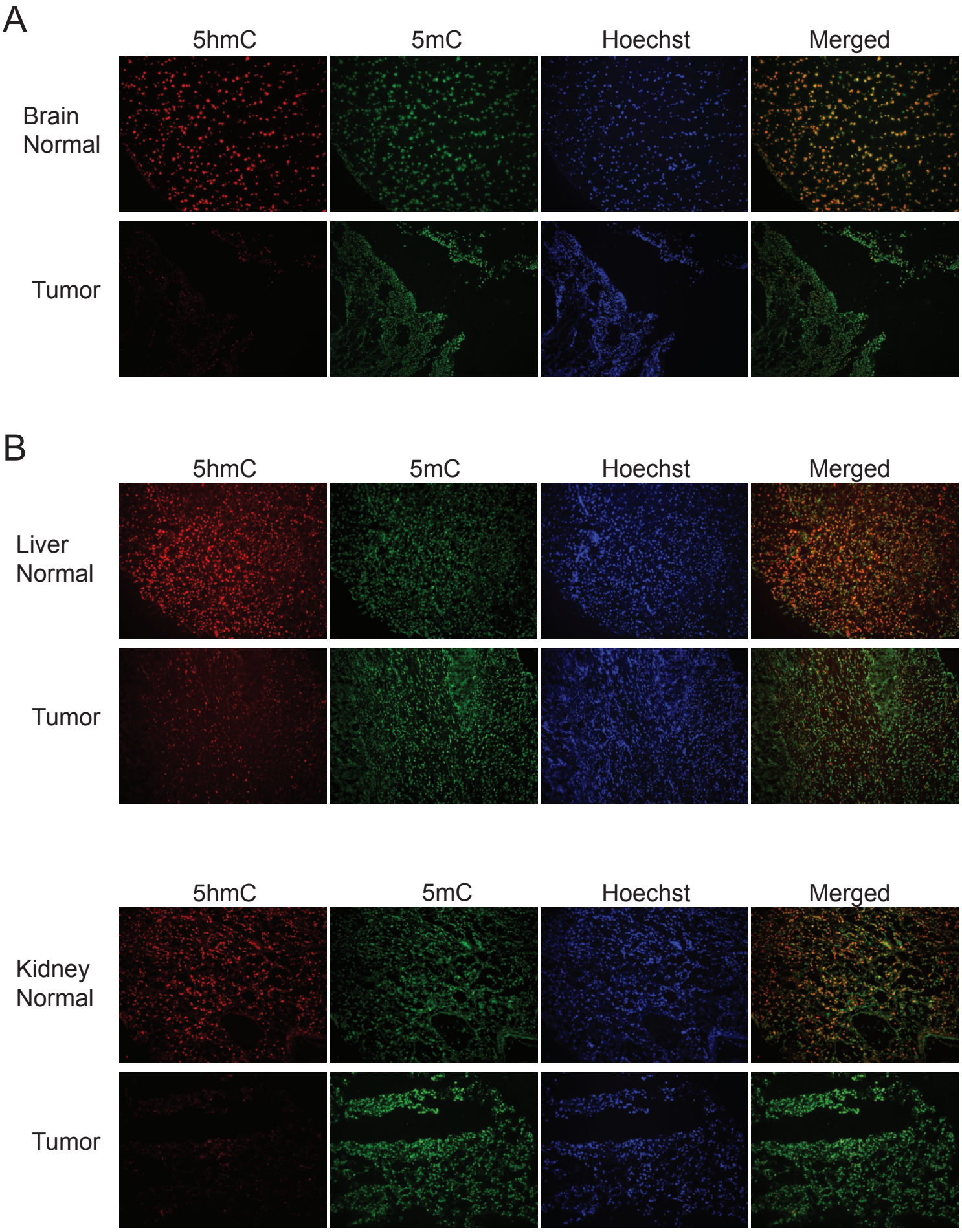

Supplementary Fig. S11

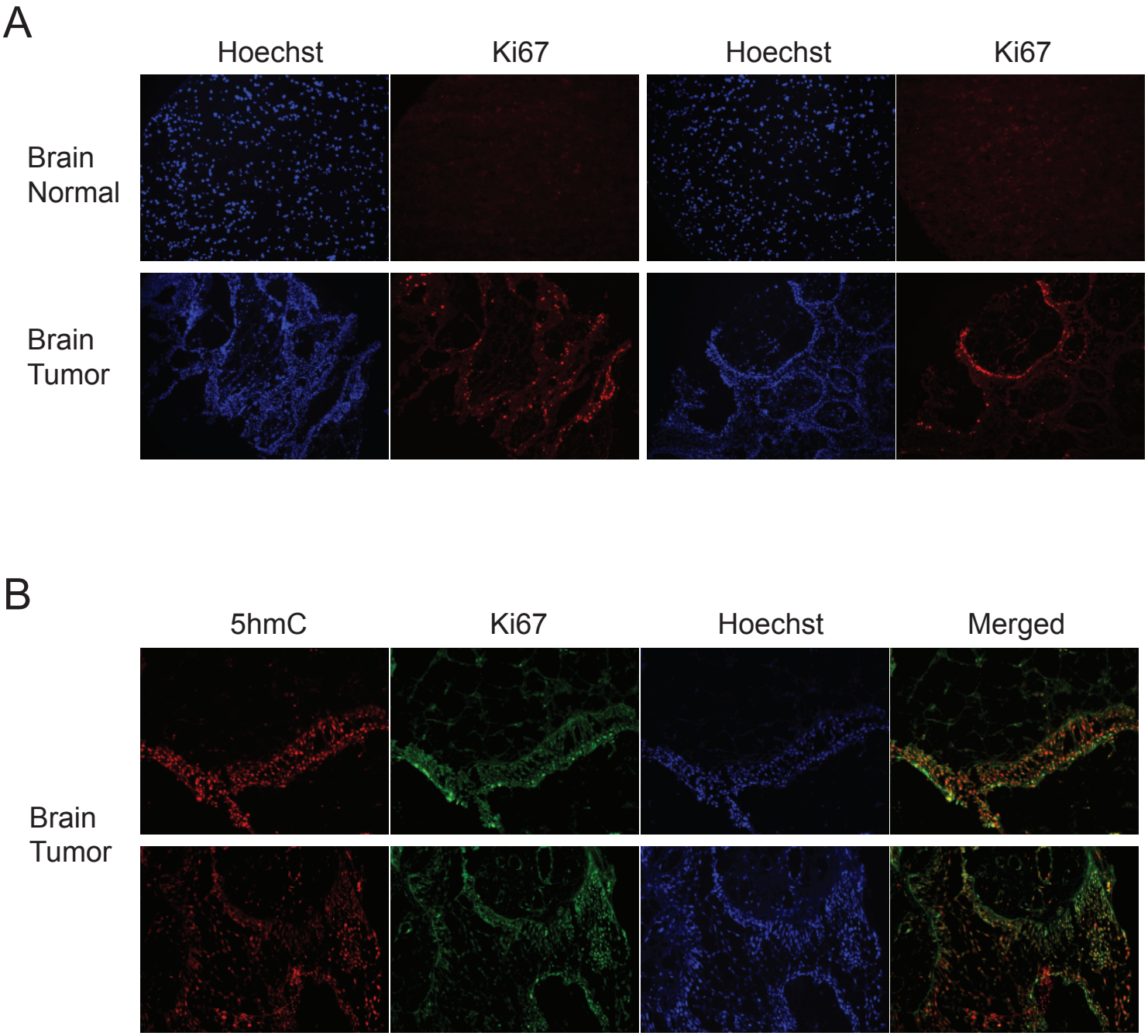

Supplementary Fig. S12

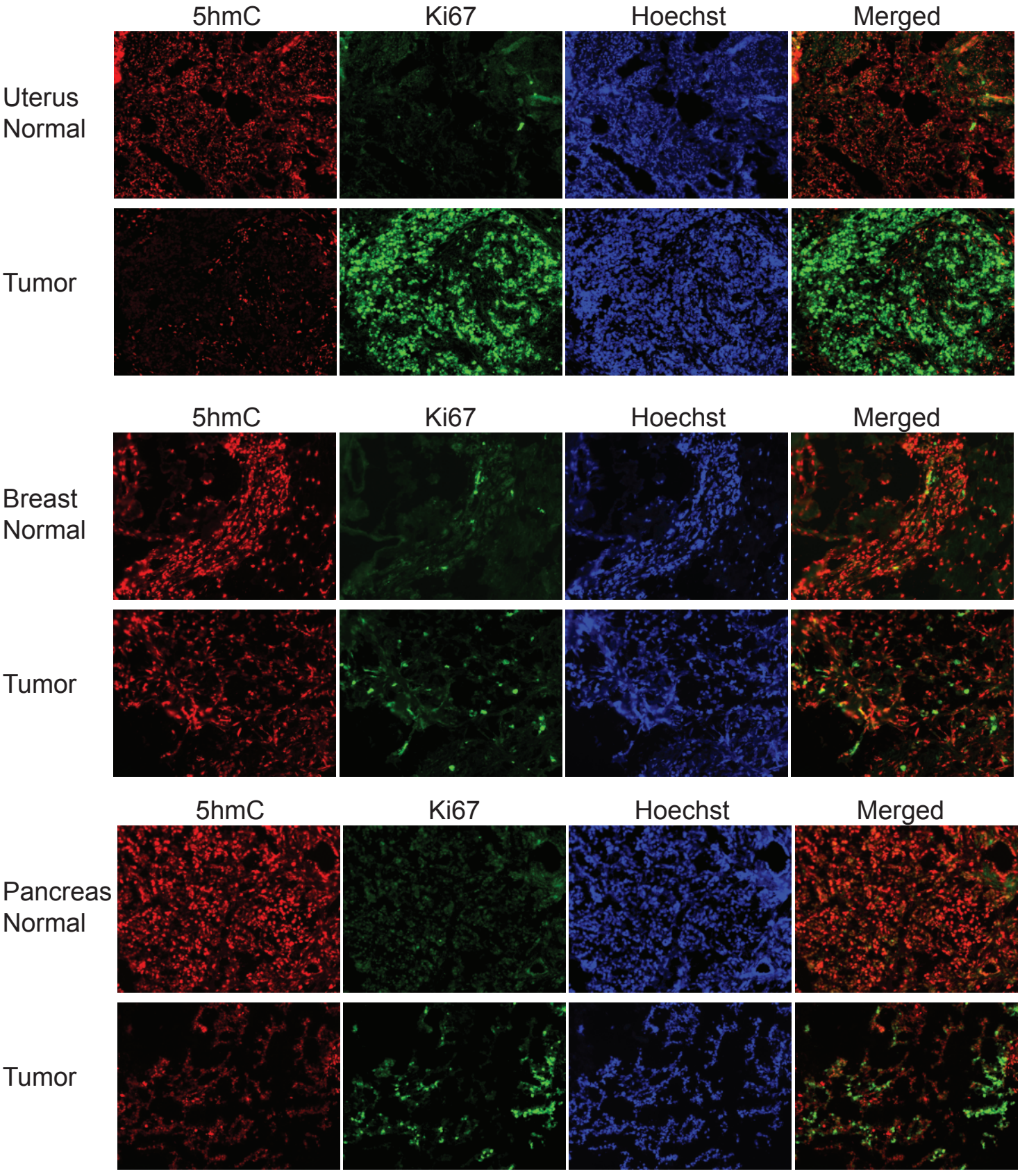

Suppementary Fig. S13

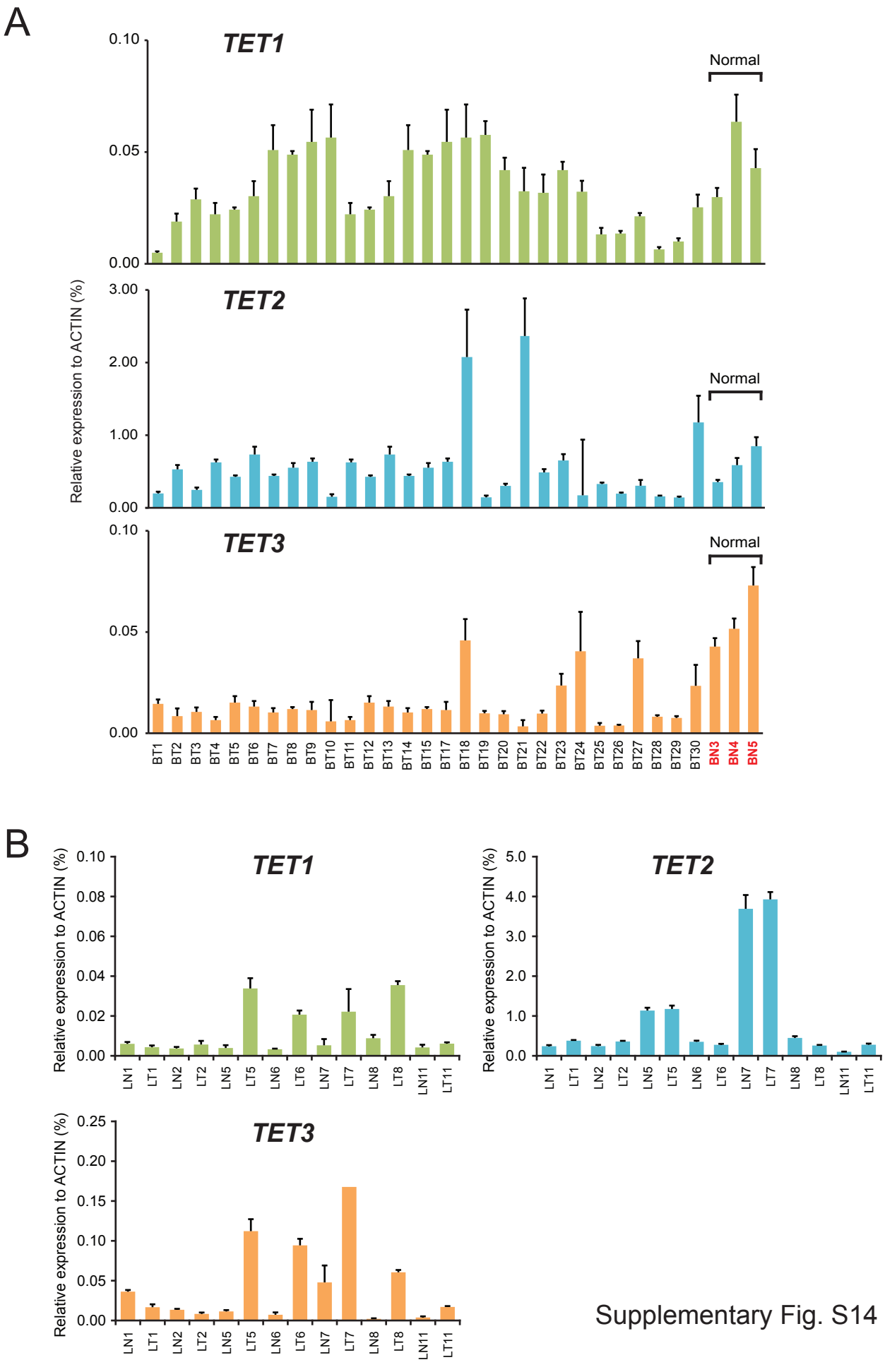

Supplementary Fig. S14